2014 5th IEEE RAS & EMBS International Conference on
Biomedical Robotics and Biomechatronics (BioRob)
August 12-15, 2014. São Paulo, Brazil

Muscle Group Activation Estimation in Human Leg during Gait Using Recursive Least Squares Embodying Hill's Muscle Model

Yunha Kim[1] and Yoichi Hori[2]

Abstract— **This paper presents a novel estimation method for extracting the activation rate of the human leg muscles using the recursive least squares algorithm. It is shown that the output force of each leg muscle group can be simply estimated from the reconstructed real measurement data. The estimation result turned out to be fairly comparable to those from electromyography, yet much simpler and faster. Considering the importance of the knowledge regarding the activation and deterioration state of each leg muscle group for rehabilitation, the proposed method is expected to contribute to the progress in the fields of biomechanics, by providing a simple, accurate, and fast estimation data to the developers, which will lead to the controller design of adaptive type walking assist devices.**

I. INTRODUCTION

World's population is rapidly getting old [1]. With continually increasing life expectancies and decreasing birth rates, many issues regarding aging are rising in importance in many societies around the world. Concerns regarding incidences of age-related pathologies are a part of the issues. In treating those patients, rehabilitating them, and helping them to return to their daily lives and enjoy them, robot technologies and applications have contributed enormously, and their missions are expected to grow in importance. In an attempt to deal with these issues, there are robots that are attached to physically disabled patients on their disabled parts of body. Especially, walking assist devices help them at a very fundamental level, considering the importance of walking ability in human life. Due to the fact that walking ability is essential for quality of life and participation in social and economic activities, gait disorders eventually disturb the patients' life itself. As the world population becomes older, the demand for such devices is increasing and expected to grow more. Moreover, not only the patients suffering from age-related pathologies involving gait disorders, such as Parkinson's Disease and the stroke, but also the young patients who have gait disorders caused by congenital and acquired diseases are the beneficiaries.

Many walking assist devices have been introduced and commercialized to rehabilitate the patients, and help them to return to their daily life activities. For example, the AlterG Bionic Leg of AlterG Inc. is well know for its performance improving the mobility of stroke patients. ReWalk is also a well known personal exoskeletal rehabilitation system, which allows the user to sit, stand, turn, and climb and descend stairs. Some other works of the field show the increasing interests in the interaction between the patient and the robotic system utilizing combined sensors and actuators as in [2] and [3]. They measure the force and torque of the user's body, and decide whether and how to augment them — in most cases simply amplifying them — which is inherently an indirect way, compared to the ones based on the segmental characteristics of the human body beforehand.

However, studies on the intrinsic characteristics the human limbs and relating them to the assist devices, are relatively few in the literature considering the substantial importance. Meanwhile, there are a number reported research works that tried identifying the parameters using external measurements, Hatze [4] first showed in 1981 that the external information of constraint forces and moments along with the human body dynamics could make the system of equations overdetermined, which enabled Vaughan et al. [5] to estimate the segmental parameters of the human body. More recently, many other researchers, including Li et al. [6] and [7], have worked on model-based estimation of segmental muscle forces during movements, yet the complexity of the estimation scheme costs much.

This work presents a simple and fast method to improve accuracy and repeatability in estimating the segmental muscle forces of the human leg during walking using the inverse dynamics embodying Hill's muscle model, with only the external measurements: the angular displacements of the hip, knee, ankle joints along with time; and the ground reaction forces. This analysis enables the simple diagnosis of a patient about his/her muscle deterioration, and the deviation from the normal muscle group activation during the gait. Consequently, the results can be used for the gait rehabilitation, and the advanced walking assist device control.

II. MUSCLES

In this section, muscles in the scope of this work are defined, and modeled by adopting Hill's three-element muscle model which has been widely used in the field of biomechanics as a standard model.

A. Muscles in Scope and Groups

In order to make the problem simple and clear, the walking motion is assumed limited in the sagittal plane, consisting of the vertical downward (x-) and the horizontal forward (y-direction), leaving 23 muscles in scope, which are gluteus maximus (GM), iliacus (IA), pectineus (PC), psoas major (PM), tensor fasciae latae (TFL), rectus femoris (RF), biceps

[1]Yunha Kim is with the Graduate School of Engineering, the University of Tokyo, 7-3-1 Hongo, Bunkyo-ku, Tokyo, Japan yunha.kim@hori.k.u-tokyo.ac.jp

[2]Yoichi Hori is with the Graduate School of Frontier Sciences, the University of Tokyo, 5-1-5 Kashiwanoha, Kashiwa-shi, Chiba, Japan hori@ieee.org

TABLE I

HUMAN LOWER LIMB MUSCLE PARAMETERS IN SCOPE [8]

Muscles	Group	PCSA [cm^2]	θ_m [deg]	d [cm]	F_{Cmax} [N]	l_0 [cm]
GM	e1	30.4	21.9	6.5	1852.6	15.7
IA	f1	10.2	14.3	5	621.9	10.7
PC	f1	1.8	0.0	5	177.0	13.3
PM	f1	7.9	10.7	5	479.7	11.7
TFL	f1	1.8	3.0	5	155.0	9.5
RF	e12	13.9	5.0	5, 4	848.8	7.6
BF	f12	16.8	12.0	6.5, 4	1021.0	11.0
GR	f12	2.3	8.2	6.5, 4	137.3	22.8
SM	f12	19.1	15.1	6.5, 4	1162.7	6.9
ST	f12	4.9	12.9	6.5, 4	301.9	19.3
SA	x12	1.9	1.3	5, 4	113.5	40.3
VI	e2	16.8	4.5	4	1024.2	9.9
VL	e2	37.0	18.4	4?	2255.4	9.9
VM	e2	23.7	29.6	4	1443.7	9.7
PP	f2	2.0	0.0	4	176.4	3.1
GN	f23	31.3	11.0	4, 5	1814.4	5.5
EDL	e3	5.7	10.8	5	345.4	6.9
FDL	e3	4.5	13.6	5	274.4	4.5
FHL	e3	7.2	16.9	5	436.8	5.3
SO	e3	58.0	28.3	5	3585.9	4.4
TP	e3	14.8	13.7	5	905.6	3.8
EHL	f3	2.7	9.4	5	436.8	5.3
TA	f3	11.0	9.6	4	673.7	6.8

femoris (BF), gracilis (GR), semimembranosus (SM), semitendinosus (ST), sartorius (SA), vastus intermedius (VI), vastus lateralis (VL), vastus medialis (VM), popliteus (PP), gastrocnemius (GN), extensor digitorum longus (EDL), flexor digitorum longus (FDL), flexor hallucis longus (FHL), soleus (SO), tibialis posterior (TP), extensor hallucis longus (EHL), and tibialis anterior (TA). This assumption is base on the idea that the forces and the moments related to lateral motion are symmetric over the sagittal plane. These 23 muscles that have force components in the sagittal plane are shown and categorized in Table I. Then they are modeled into a multi-link mechanical structure, where each muscle has joints and moment arm to act on. The parameters are collected from [8], which are based on anatomical measurements and normalization.

Fig. 1 shows the schematic view of the assumed multi-link structure. The 23 muscles are sorted into 10 categories according to their acting joints and working direction, based on the fact that the lumped force output characteristics of the muscles vastly depend on the direction of the attachment and the number of the joint-link they involve [9][10], which are: e_1 and f_1, the extensors and flexors at the hip joint (J1); e_2 and f_2, the extensors and flexors at the knee joint (J2); e_3 and f_3, the extensors and flexors at the ankle joint (J3); e_{12}, the bi-articular muscles that bend the hip and at the same time extend the knee; f_{12}, the bi-articular muscles that extend the hip and at the same time bend the knee; x_{12}, the bi-articular muscles that bend the hip and at the same time bend the knee; and f_{23}, the bi-articular muscles that bend the knee and at the same time extend the ankle outwards. Specific names and the categories of the 23 muscles are indicated in Table I.

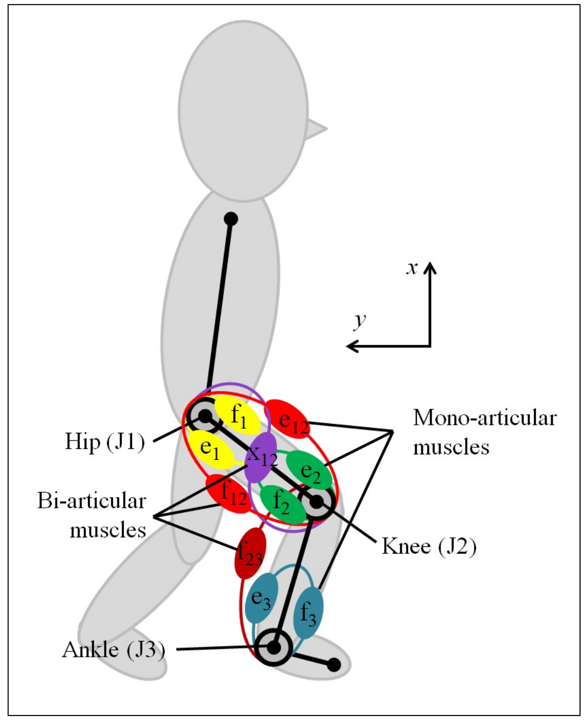

Fig. 1. 10 categories of a human leg muscles. e_1 and f_1 are the mono-articular extensor and flexor muscles for the hip joint, e_2 and f_2 are the mono-articular extensor and flexor muscles for the knee joint, and e_3 and f_3 are the mono-articular extensor and flexor muscles for the ankle joint. e_{12}, f_{12}, f_{23}, and x_{12} are the bi-articular muscles that exert the same amount of torque to their adjacent joints.

B. Hill's Muscle Model

Hill's three-element muscle model has been widely adopted for describing muscle behavior, and has become a standard in the field of biomechanics. For the estimation in this work, Hill's is used to model the muscles in scope. The model describes the muscle-tendon unit (MTU) force with three different elements, which are the contractile element (CE), the parallel element (PE), and the series element (SE). The force that an MTU produce is written as follows.

$$F_{MTU} = F_{CE} + F_{PE} \tag{1}$$
$$F_{SE} = F_{CE} \tag{2}$$

where, the transient characteristics of F_{SE} can be neglected assuming that the stiffness of a tendon is high enough. Then, an MTU can be modeled with only F_{CE} and F_{PE}, which are written as follows.

$$F_{CE} = f_{Cv} \cdot f_{Cl} \cdot F_{Cmax} \cdot a_m \cdot \cos\theta_m \tag{3}$$
$$F_{PE} = f_{Pl} \cdot F_{Pmax} \cdot \cos\theta_m + f_{Pv} \tag{4}$$

where, a_m is the activation level of the contractile element of the MTU which has a value between 0 and 1, θ_m is the pennation angle of the muscle fiber, and F_{Cmax} and F_{Pmax} are the maximal contractile force and the maximal isometric force, respectively, which are all constants. f_{Cv}, f_{Cl}, f_{Pl}, and f_{Pv} are the nonlinear functions of the muscle velocity (v) and the muscle length (l), which are defined as below.

$$f_{Cv} = \frac{0.143}{0.107 + \exp\left(-1.41 \sinh\left(\frac{3.20v}{v_{max}} + 1.60\right)\right)} \quad (5)$$

$$f_{Cl} = \exp\left(-0.5\left(\frac{l/l_0 - 1.05}{0.19}\right)^2\right) \quad (6)$$

$$f_{Pl} = \frac{\exp\left(10\left(l/l_0 - 1\right)\right)}{148.41} \quad (7)$$

$$f_{Pv} = -Bv^2 \quad (8)$$

where, v_{max} is the maximal contractile velocity of a muscle which is known to be around 0.50 m/s [11], l_0 is the resting length of the muscle fiber, and every coefficient in the equations is empirically given by [12] and [13].

In addition, each muscle has different maximal force output, and consequent torque according to the place of attachment, the physiological cross-section area (PCSA), and the length of moment arm d. These parameters vary from person to person and even according to the posture. However in this work, an average subject, who is 172cm tall with 70kg body mass and the average body proportion, is assumed for simplicity, and the postural variation is neglected regarding that it is relatively small. Then these parameters can be assumed constant, as given in Table I.

III. Human Body Joint-Link Model

Then, the muscle model introduced in the previous section is embedded into the joint-link model of the human body, to formulate the estimation algorithm. In this work, a human body is modeled to consist of 4 links with correspondent masses, which are connected via 3 joints as schematically shown in Fig. 1.

A. Equations of Motion

Assuming that there exists no external force nor moment other than the ground reaction force (F_{GRF}) applied to the subject, the equation of motion of a leg in scope during normal walking is written as follows, regardless of the number of supporting legs: single or double support phases, i.e. during double support phase, two equations for each leg are superpositioned with the smooth transition assumption [14]. The frame of reference is assumed attached at the hip joint for the description.

$$M\ddot{\Theta} + C + G + RF_{MTUs} + J^T F_{GRF} = 0 \quad (9)$$

for one leg in scope, where, Θ is the angular displacement vector of the three joints of the two legs, $M(\Theta)$ is the mass and inertia matrix, $C(\Theta, \dot{\Theta})$ is the Coriolis terms, $G(\Theta)$ is the gravitational terms, $R(\Theta)$ is the muscle embedding transformation, F_{MTUs} is the force output vector of the muscle-tendon units, $J(\Theta)$ is the Jacobian, and lastly F_{GRF} is the ground reaction force vector. To be specific, these terms are written as follows.

$$\Theta = [\theta_1 \ \theta_2 \ \theta_3]^T \quad (10)$$

$$M(\Theta) = \begin{bmatrix} M_{11} & M_{12} & M_{13} \\ M_{21} & M_{22} & M_{23} \\ M_{31} & M_{32} & M_{33} \end{bmatrix} \quad (11)$$

$$C(\Theta, \dot{\Theta}) = [C_1 \ C_2 \ C_3]^T \quad (12)$$

$$G(\Theta) = [G_1 \ G_2 \ G_3]^T \quad (13)$$

$$R(\Theta) = \begin{bmatrix} R_{11} & R_{12} & \dots & R_{123} \\ R_{21} & R_{22} & \dots & R_{223} \\ R_{31} & R_{32} & \dots & R_{323} \end{bmatrix} \quad (14)$$

$$F_{MTUs}(\Theta, \dot{\Theta}) = [F_{MTU1} \ F_{MTU2} \ \dots \ F_{MTU23}]^T \quad (15)$$

$$J(\Theta) = \begin{bmatrix} J_{11} & J_{12} & J_{13} \\ J_{21} & J_{22} & J_{23} \end{bmatrix} \quad (16)$$

$$F_{GRF} = \begin{bmatrix} f_x \\ f_y \end{bmatrix} \quad (17)$$

where,

$$M_{11} = \frac{m_2 l_1^2}{4} + I_2 + (m_3 + m_4) l_1^2 \quad (18)$$

$$M_{12} = M_{21} = \left(\frac{m_3 l_1 l_2}{2} + m_4 l_1 l_2\right) \cos(\theta_2 - \theta_1) \quad (19)$$

$$M_{13} = M_{31} = \left(\frac{m_4 l_1 l_3}{2}\right) \cos(\theta_3 - \theta_1) \quad (20)$$

$$M_{22} = \frac{m_3 l_2^2}{4} + I_3 + m_4 l_2^2 \quad (21)$$

$$M_{23} = M_{32} = \left(\frac{m_4 l_2 l_3}{2}\right) \cos(\theta_3 - \theta_2) \quad (22)$$

$$M_{33} = \frac{m_4 l_3^2}{4} + I_4 \quad (23)$$

$$\begin{aligned} C_1 = &-\left(\frac{m_3 l_1 l_2}{2} + m_4 l_1 l_2\right) \dot{\theta}_2^2 \sin(\theta_2 - \theta_1) \\ &-\left(\frac{m_4 l_1 l_3}{2}\right) \dot{\theta}_3^2 \sin(\theta_3 - \theta_1) \quad (24) \\ C_2 = &\left(\frac{m_3 l_1 l_2}{2} + m_4 l_1 l_2\right) \dot{\theta}_1^2 \sin(\theta_2 - \theta_1) \\ &-\left(\frac{m_4 l_2 l_3}{2}\right) \dot{\theta}_3^2 \sin(\theta_3 - \theta_2) \quad (25) \\ C_3 = &\left(\frac{m_4 l_1 l_3}{2}\right) \dot{\theta}_1^2 \sin(\theta_3 - \theta_1) \\ &+\left(\frac{m_4 l_2 l_3}{2}\right) \dot{\theta}_2^2 \sin(\theta_3 - \theta_2) \quad (26) \end{aligned}$$

$$G_1 = -gc_1\left(m_1 h\right) \tag{27}$$

$$G_2 = -gc_2\left(m_1 l_1 + \frac{m_2 l_1}{2}\right) \tag{28}$$

$$G_3 = -gc_3\left(m_1 l_2 + m_2 l_2 + \frac{m_3 l_2}{2}\right) \tag{29}$$

$$R_{ij} = \pm \epsilon d_i \tag{30}$$

where, $\epsilon = 1$ if muscle j works on the joint i, otherwise $\epsilon = 0$. Sign of R_{ij} depends on the direction of the torque the muscle j exert on the joint i.

$$J_{11} = -l_1 s_1 - l_2 s_{12} - l_3 s_{123} \tag{31}$$

$$J_{12} = -l_2 s_{12} - l_3 s_{123} \tag{32}$$

$$J_{13} = -l_3 s_{123} \tag{33}$$

$$J_{21} = l_1 c_1 + l_2 c_{12} + l_3 c_{123} \tag{34}$$

$$J_{22} = l_2 c_{12} + l_3 c_{123} \tag{35}$$

$$J_{23} = l_3 c_{123} \tag{36}$$

where, $s_i = \sin\theta_i$, $c_j = \cos\theta_j$, $s_{ij} = \sin(\theta_i + \theta_j)$, and $c_{ijk} = \cos(\theta_i + \theta_j + \theta_k)$, respectively, and the corresponding parameters used in the estimation algorithm are shown in Table II [15]. Where, the foot link length l_3 is assumed to be proportional to the step cycle to have 0 at hill-strike and l_3 at toe-off in the model.

TABLE II

PARAMETERS OF HUMAN BODY JOINT-LINK MODEL [15]

Symbol	Meaning	Value [Unit]
I_1	Upper Body Inertia Mnt	2.87 [kgm^2]
I_2	Upper Leg Inertia Mnt	0.112 [kgm^2]
I_3	Lower Leg Inertia Mnt	0.051 [kgm^2]
I_4	Foot Inertia Mnt	0.006 [kgm^2]
m_1	Upper Body Mass	47.46 [kg]
m_2	Upper Leg Mass	7.00 [kg]
m_3	Lower Leg Mass	3.26 [kg]
m_4	Foot Mass	1.02 [kg]
l_1	Upper Leg Link Length	0.421 [m]
l_2	Lower Leg Link Length	0.423 [m]
l_3	Foot Link Length	0.261 [m]
g	Gravitational Aceel.	9.81 [m/s^2]

B. Estimation Algorithm Embodying Hill's Muscle Model

As briefly shown above, one of the keys for the estimation is the use of nonlinear muscle model in the human body dynamics. The equations introduced above are transformed into the estimation algorithm, which is recursive least squares in this work. The formulation is as follows. Splitting F_{MTUs} into F_{CEs} and F_{PEs}, then equation (9) becomes

$$M\ddot{\Theta} + C + G + RF_{CEs} + RF_{PEs} + J^T F_{GRF} = 0 \tag{37}$$

then, substituting equation (3), it becomes

$$R\left[f_{Cvi} f_{Cli} F_{Cmaxi}\right] A_m = -\left[M\ddot{\Theta} + C + G + RF_{PEs} + J^T F_{GRF}\right] \tag{38}$$

where, $[f_{Cvi} f_{Cli} F_{Cmaxi}]$ is the muscle grouping matrix (23×10), and A_m is the muscle group activation rate vector (10×1) which is estimated. Further formulation for the estimation algorithm follows in the next section.

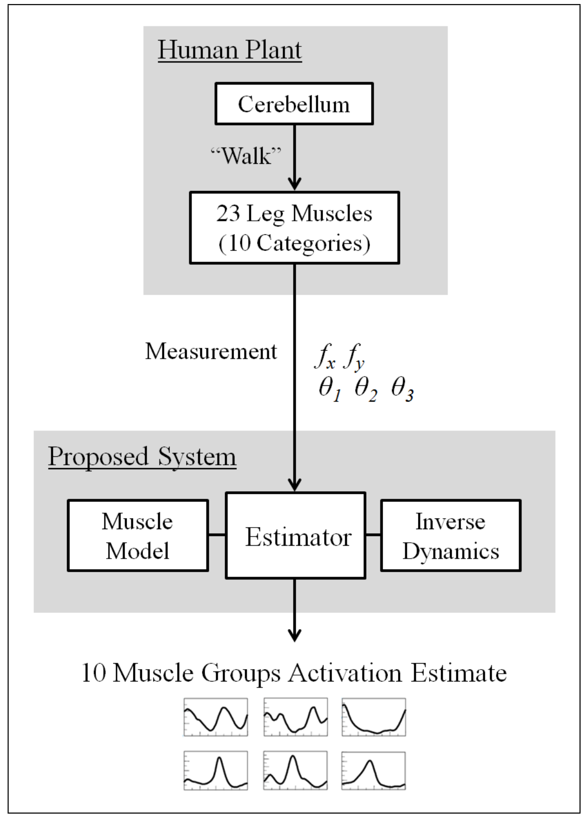

Fig. 2. Schematic flow of the proposed method.

IV. MUSCLE GROUP ACTIVATION ESTIMATION

In this section, using the model elaborated in the previous section, the individual muscle group activation rates are estimated.

A. Schematic Flow

As shown in Fig. 2, when people walk, the outputs, which are easily measurable, are the joint angles and the ground reaction forces, using encoders and force sensors. The point of this work is to estimate the inputs from 23 actuators in 10 groups–muscles in human plant, by only using those external measurements. The schematic flow of this work consists of the data reconstruction, and the estimation of the individual muscle group activation rates using the least squares algorithm. Then the estimation results are compared with evidences from EMG signal measurements and verified in the following sections.

B. Measurement Data Reconstruction

The external measurement signals used in this work, are reconstructed ones based on findings of the literature. The angular displacement profiles of the hip, knee, and ankle joints, and the ground reaction force profiles are stacked with time, and fed into the estimation algorithm.

The angular displacements of the human lower limb joints are reconstructed based on the measurement data from [16], and the ground reaction force profiles are reconstructed using the measured data in [17]. Standard deviation originating

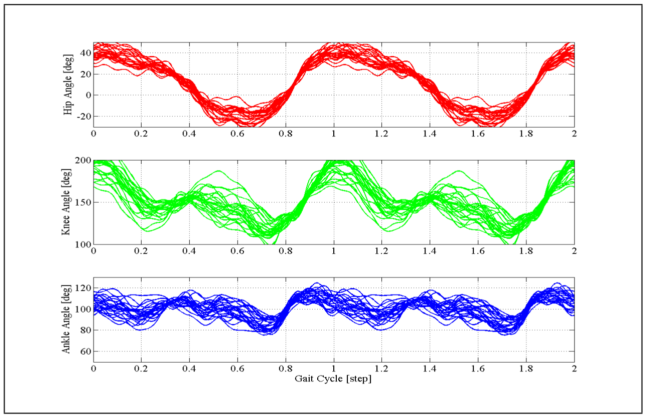

Fig. 3. Reconstructed joint angle displacements of the average normal subject during walking. Hip angle (upper), knee angle (middle), and ankle angle (lower) are shown with respect to the gait cycle.

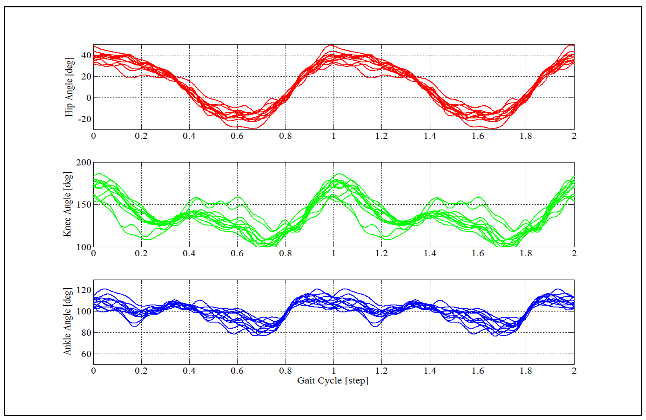

Fig. 4. Reconstructed joint angle displacements of the average patient with knee disease during walking.

from multiple subjects and trials of the measurements is reflected in the reconstructed signals, which are stacked and synchronized along with time, and normalized to meet the average subject assumption. The reconstructed joint angle displacements are shown in Fig. 3 for the average normal subject and 4 for the average patient, and the reconstructed ground reaction forces are shown in Fig. 5 for the average normal subject and 6 for the average patient with knee disease. Throughout the estimation scheme, a normal walking, which is characterized by approximately 1.2 m/s and 105 steps per minute, is assumed. Parameters used in the algorithm comply with those in Table I and II.

C. Algorithm: the Recursive Least Squares

For the estimation the recursive least squares method is used. Using the reconstructed measurements of Fig. 3∼6 and equation (38), the muscle group activation matrix A_m 10×1 is estimated. Where,

$$A_m = \left[\begin{array}{cccc} a_{m1} & a_{m2} & \dots & a_{m10} \end{array} \right] \tag{39}$$

and $0 \leq a_{mi} \leq 1$. The estimate vector A_m is calculated at every 1 ms with the window of 60 samples, and plotted with regard to time.

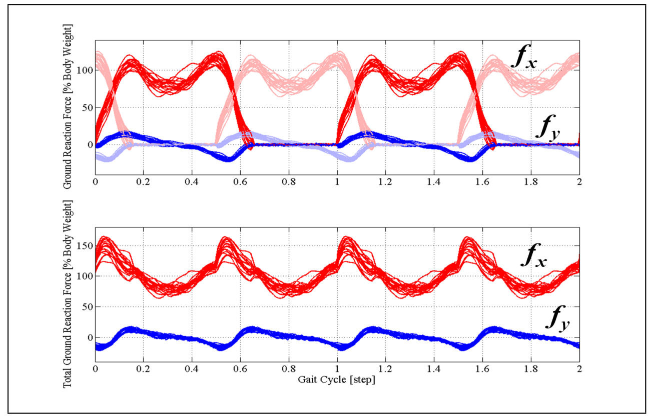

Fig. 5. Reconstructed ground reaction forces (GRF) of the average normal subject during walking. Vertical component of GRF in red has larger in amplitude than horizontal component in blue. GRFs of both legs are shown in the upper graph, and the sum of the two is shown in the lower with respect to the gait cycle.

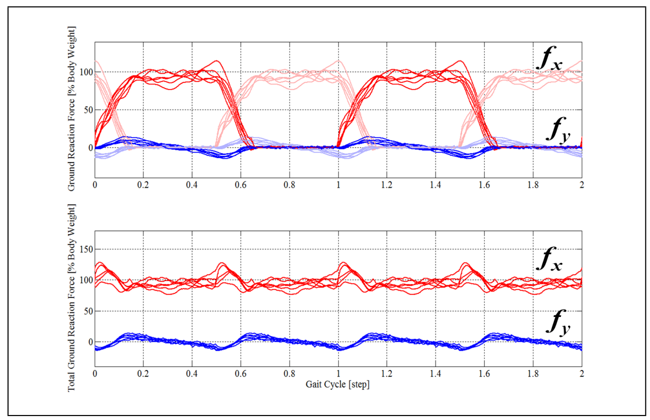

Fig. 6. Reconstructed ground reaction forces (GRF) of the average patient with knee disease during normal walking.

V. Results and Discussion

The estimation results from the proposed algorithm are compared to the measurement data using EMG (electromyographic) signal. The patterns from [18] are used for the main reference of the comparison. As shown in Fig. 7, the estimation result of the average normal subject is fairly comparable to the EMG measurement results, which supports the validity of the estimation. And in Fig. 8, it is shown that the patient's muscle activation deteriorated with low activation levels for all muscle groups.

However, the accuracy of the estimation should be enhanced via refinement. Moreover, the external measurement data used in this work was collected from multiple previous works, which fundamentally lacks consistency. Data gathering from a single experiment is needed; experiments should be done, and the effectiveness of the proposed method needs to be further shown.

VI. Conclusion

A simple and fast estimation method for extracting the activation rate of the human leg muscle groups using the recursive least squares embodying Hill's muscle model is

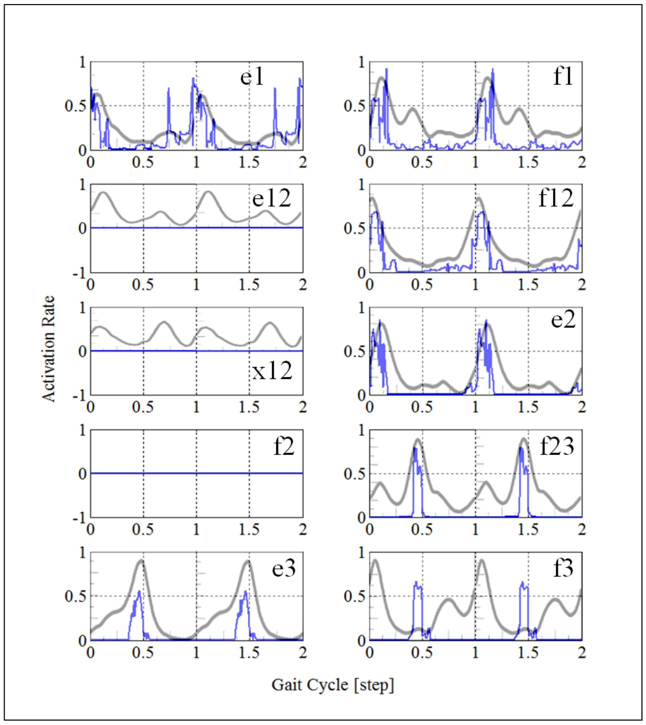

Fig. 7. Estimated results of the human leg muscle group activation rate of the average normal subject. From the top left to the right and then to the bottom, the activation rates of 10 muscle groups labeled in Table I are shown. The transparent gray lines indicate the EMG measurements [18] of the representative muscles of the corresponding groups.

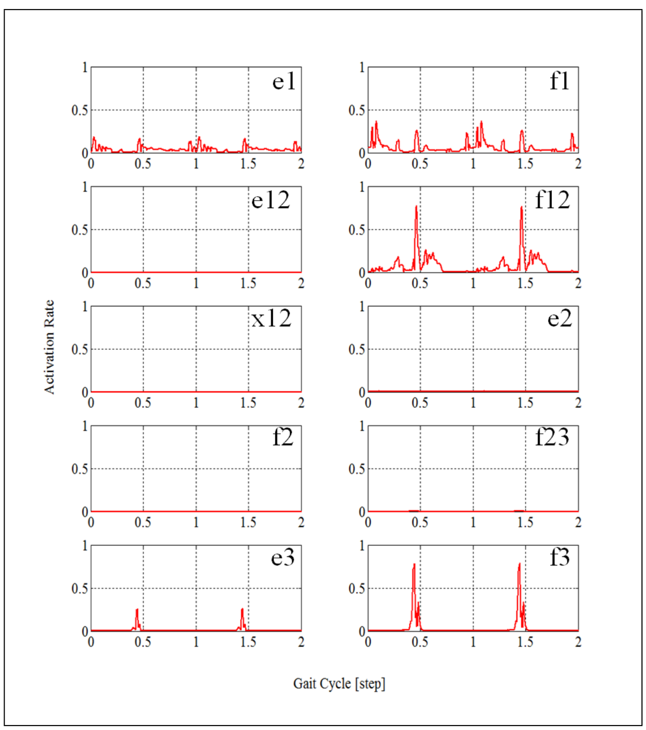

Fig. 8. Estimated results of the human leg muscle group activation rate of the average patient. From the top left to the right and then to the bottom, the activation rates of 10 muscle groups labeled in Table I are shown.

proposed. The output force of each leg muscle group can be simply estimated. The estimation result is fairly comparable to those from electromyography, yet much simpler and less invasive. Considering the importance of the knowledge regarding the activation and deterioration state of leg muscles, the proposed method is expected to contribute to the progress in helping patients with gait problems, by providing a simple, accurate, and less invasive estimation data to the developers. Our future work will include the enhancement of the estimation accuracy, the verification of the proposed method with real-time measurements and estimation, which will eventually lead to the controller design of adaptive type walking assist devices.

REFERENCES

[1] Population Division of the Department of Economic and Social Affairs of the United Nations Secretariat, "World Population Prospects: The 2012 Revision," August 2013

[2] J. A. Blaya and H. Herr, "Adaptive control of a variable-impedance ankle-foot orthosis to assist drop-foot gait," *IEEE Trans. on Neural System Rehabilitation Engineering*, Vol.12, pp.24-31, 2004

[3] K. E. Gordon, G. S. Sawicki, and D. P. Ferris, "Mechanical performance of artificial pneumatic muscles to power an ankle-foot orthosis," *Journal of Biomechanics*, Vol.39, pp.1831-1841, 2006

[4] H. Hatze, "A comprehensive model for human motion simulation and its application to the take-off phase of the long jump," *Journal of Biomechanics*, Vol.14, pp.833-843, 1981

[5] C. L. Vaughan, J. G. Andrews, and J. G. Hay, "Selection of body segment parameters by optimization methods," *Journal of Biomechanical Engineering*, Vol.104, pp.38-44, 1982

[6] G. Li, K. R. Kaufman, E. Y. Chao, and H. E. Rubash, "Prediction of antagonistic muscle forces using inverse dynamic optimization during flexion/extension of the knee," *Journal of Biomechanical Engineering*, Vol.121, pp.316-322, 1999

[7] A. D. Kuo, "A least squares estimation approach to improving the precision of inverse dynamics computations," *Journal of Biomechanics*, Vol.120, No.1, pp.148-159, 1998

[8] E. M. Arnold, S. R. Ward, R. L. Lieber, and S. L. Delp, "A Model of the Lower Limb for Analysis of Human Movement," *Annals of Biomedical Engineering*, Vol.38, No.2, pp.269-279, 2010

[9] T. Fujikawa, T. Oshima, M. Kumamoto, and N. Yokoi, "Output force at the endpoint in human upper extremities and coordinating activities of each antagonistic pairs of muscles," *Trans. Japan Society of Mechanical Engineers, C*, Vol.65, No.632, pp.1557-1564, 1999

[10] M. Kumamoto, T. Oshima, and T. Yamamoto, "Control properties induced by the existence of antagonistic pairs of bi-articular muscles – Mechanical engineering model analyses," *Human Movement Science*, Vol.13, No.5, pp.611-634, 1994

[11] J. J. Widrick, J. G. Romatowski, M. Karhanek, and R. H. Fitts, "Contractile properties of rat, rhesus monkey, and human type I muscle fibers," *Am. Journal of Physiology*, Vol.272, pp.R34-R42, 1997

[12] J. Rosen, M. B. Fuchs, and M. Arcan, "Performances of Hill-Type and Neural Network Muscle Models – Toward a Myosignal-Based Exoskeleton," *Computers and Biomedical Research*, Vol.32, pp.415-439, 1999

[13] L. Schutte, "Using musculoskeletal models to explore strategies for improving performance in electrical stimulation-included leg cycle ergometry," *Ph.D. dissertation*, Stanford University, CA, USA, 1992

[14] L. Ren, R. K. Jones, and D. Howard, "Whole body inverse dynamics over a complete gait cycle based only on measured kinematics," *Journal of Biomechanics*, Vol.41, pp.2750-2759, 2008

[15] I. P. Herman, "Physics of the Human Body (Biological and Medical Physics, Biomedical Engineering)," Springer, 2007

[16] A. Cappozzo, T. Leo, and A. Pedotti, "A General Computing Method for the Analysis of Human Locomotion," *Journal of Biomechanics*, Vol.8, pp.307-320, 1974

[17] E. Schneider and E. Y. Chao, "Fourier analysis of ground reaction forces in normals and patients with knee joint disease," *Journal of Biomechanics*, Vol.16, No.8, pp.591-601, 1983

[18] Y. P. Ivanenko, R. E. Poppele, and F. Lacquaniti, "Five basic muscle activation patterns account for muscle activity during human locomotion," *Journal of Physiology*, Vol.556, No.1, pp.267-282, 2004